ISBN 978-989-9121-59-1
57th LISBON Global Congress on "Chemical, Biological, Environment & Medical Sciences" (LCBEM-25)
Dec. 10-12, 2025 Lisbon (Portugal)

Optimizing Calcium Hydroxide Treatment for Multi-Contaminant Removal in Municipal Wastewater

[1]Leon M Mudau, Prof Elvis Fosso-Kankeu, Prof Antoine F Mulaba-Bafubiandi, Dr Alseno K Mosai

[1]Mineral Processing and Technology Research Centre, Department of Metallurgy, School of Mining, Metallurgy and Chemical Engineering, Faculty of Engineering and The Built Environment, University of Johannesburg, PO Box 17911, Doornfontein, Johannesburg 2028, South Africa
[2]Department of Chemistry, University of Pretoria, Pretoria, South Africa
[3] Faculte des Sciences Appliquees, Universite de Mbuji-Mayi, BP 225, Mbuji-Mayi, Kasai Orientale, Republique Democratique du Congo

Abstract: *This study examines the use of calcium hydroxide [$Ca(OH)_2$] as an alkaline treatment agent for the simultaneous removal of phosphate and metal ions from municipal wastewater. A series of batch experiments was conducted to optimize $Ca(OH)_2$ dosage, mixing speed, and contact time, with pH monitored to understand system behavior and precipitation dynamics. Increasing $Ca(OH)_2$ dosage elevated pH substantially, promoting phosphate removal through the formation of calcium phosphate. Metal ion removal similarly improved at higher pH levels, where hydroxide precipitation becomes thermodynamically favorable. The results demonstrate that controlled alkalization can support efficient multi-contaminant removal while minimizing chemical consumption and sludge formation. Overall, the study provides a practical framework for developing low-cost, sustainable wastewater treatment strategies that are particularly suitable for municipalities operating under resource constraints.*

Keywords: *Calcium hydroxide, Metal removal, Phosphate precipitation, Wastewater treatment optimization*

1. Introduction

Municipal wastewater (MWW) treatment plays a critical role in protecting public health and aquatic ecosystems, yet many treatment plants struggle to balance performance, cost, and sustainability. Excess nutrients such as phosphate (PO_4^{3-}) along with trace heavy metals, are key pollutants contributing to eutrophication, oxygen depletion, and toxicity in receiving water bodies [1], [2]. Conventional biological processes, such as activated sludge and nitrification, can effectively remove organic matter but often fail to achieve simultaneous removal of nutrients and metals, particularly under resource-constrained conditions [3].

Chemical precipitation using alkaline reagents such as calcium hydroxide [$Ca(OH)_2$] offers a cost-effective and robust approach to target multiple pollutants at once. When introduced into wastewater, $Ca(OH)_2$ elevates pH and promotes the formation of insoluble calcium phosphate compounds, thereby facilitating phosphate removal [4]. The increased alkalinity shifts redox conditions that can precipitate

[1] Leon M Mudau1, Alseno K Mosai[2], Elvis Fosso-Kankeu[1], Antoine F Mulaba-Bafubiandi[1,3]
[1]Mineral Processing and Technology Research Centre, Department of Metallurgy, School of Mining, Metallurgy and Chemical Engineering, Faculty of Engineering and The Built Environment, University of Johannesburg, PO Box 17911, Doornfontein, Johannesburg 2028, South Africa
[2]Department of Chemistry, University of Pretoria, Pretoria, South Africa
[3] Faculte des Sciences Appliquees, Universite de Mbuji-Mayi, BP 225, Mbuji-Mayi, Kasai Orientale, Republique Democratique du Congo

metals as hydroxides [5], [6]. These coupled reactions make lime treatment a promising method for integrated contaminant removal.

Recent studies have revisited $Ca(OH)_2$ treatment within the context of sustainable and decentralized wastewater management. For instance, it was demonstrated that lime-based precipitation in MWW significantly has been reported to reduce phosphate and metal concentrations simultaneously, highlighting its potential for integrated nutrient management [7]. It was also reported that enhanced metal removal is possible under elevated pH due to hydroxide formation and co-precipitation processes [4]. Despite these advantages, the optimization of operational parameters such as $Ca(OH)_2$ dosage, mixing speed, and contact time remains crucial to balance efficiency, sludge generation, and chemical cost.

Therefore, this study investigates the use of calcium hydroxide as a multifunctional treatment agent for the simultaneous removal of phosphate and heavy metals from MWW. By systematically evaluating the influence of dosage, mixing intensity, and reaction time, this research aims to develop an optimized and sustainable framework suitable for application in resource-limited municipal systems

2. Materials and Methods

2.1. Sample Collection and Preparation

MWW was sourced from the Zeekoegat Wastewater Treatment Works in Pretoria, South Africa with samples collected prior to any treatment stage. Each experimental run used 500 mL of wastewater placed in a 1 L glass beaker to allow adequate mixing and aeration.

2.2. Reagents and Chemicals

Analytical-grade calcium hydroxide [$Ca(OH)_2$] (≥95% purity) was procured from Sigma-Aldrich and employed as the alkaline treatment agent. Deionized water was used exclusively for the preparation of reagents and the cleaning of all laboratory glassware to ensure analytical accuracy and prevent cross-contamination. All chemicals were stored, prepared, and handled in accordance with standard laboratory safety and quality assurance protocols.

2.3. Experimental Design

A three-factor, three-level experimental design was developed using Design-Expert® software (Version 13, Stat-Ease Inc.) to evaluate the combined effects of $Ca(OH)_2$ dosage, mixing speed, and contact time on the simultaneous removal of phosphate, ammonia, and heavy metals from municipal wastewater. The selected factor levels were $Ca(OH)_2$ dosages of 0.5, 1.75, and 3.0 g/L, mixing speeds of 50, 125, and 200 rpm, and contact times of 10, 35, and 60 minutes, respectively. These levels were chosen based on preliminary optimization trials and supporting literature to represent operational conditions suitable for alkaline wastewater treatment.

The software generated a rotatable design comprising 13 experimental runs, which were randomized by Design-Expert to minimize systematic bias and account for experimental variability. Each run was conducted using 500 mL of municipal wastewater in a 1 L beaker, with the corresponding $Ca(OH)_2$ mass ranging from 0.25 g to 1.50 g, depending on the dosage level. The reagent was added directly to the wastewater, and the mixture was agitated using a magnetic stirrer at the specified speed. The contact time was recorded from the moment of reagent addition. Following treatment, the suspensions were allowed to settle for 30 minutes, after which the supernatant was collected and analyzed for water quality and contaminant concentrations.

The experimental design matrix generated by the software is presented in Table I below.

TABLE I. EXPERIMENTAL MATRIX GENERATED BY DESIGN-EXPERT® (VERSION 13, STAT-EASE INC.). THE SOFTWARE RANDOMIZED THE RUN ORDER TO MINIMIZE EXPERIMENTAL BIAS AND ENSURE STATISTICAL VALIDITY OF THE RESULTS.

Run	$Ca(OH)_2$ Dosage (g)	Mixing speed (rpm)	Contact time (min)
1	1.75	125	35
2	0.5	200	35
3	3	125	10
4	1.75	50	10
5	1.75	50	60
6	1.75	200	10
7	3	50	35
8	3	125	60
9	3	200	35
10	0.5	50	35
11	0.5	125	10
12	1.75	200	60
13	0.5	125	60

2.4. Analytical Methods

Key water quality parameters, including pH and dissolved ions were measured before and after treatment using a calibrated multiparameter probe (Hanna Instruments, USA) and analytical instruments. The concentration of phosphate (PO_4^{3-}) was determined using ion chromatography (IC) (Thermo Scientific Gallery Plus), while heavy metal and major cation concentrations (Ca, Mg, K, Na, Ni, and Zn) were quantified using atomic absorption spectroscopy (AAS) (Thermo Scientific).

2.5. Quality Control and Data Analysis

All instruments were calibrated with certified standards prior to measurement. Data management and analysis was carried out using X'Pert HighScore, Microsoft Excel and Origin. X'Pert HighScore was specifically used for analyzing X-ray diffraction (XRD) data of the solid residues after treatment. Microsoft Excel was employed for organizing raw experimental data, performing basic calculations, and generating plots. Origin was used to generate high-resolution graphs, which helped in visualizing the effect of different treatment conditions over time. This facilitated clearer interpretation of the results and supported data-driven conclusions.

3. Results & Discussion

3.1. Initial Wastewater Composition

The MWW sample was first analyzed to establish its baseline characteristics before any treatment. The water showed the typical complexity of municipal effluent, containing a mix of domestic and light industrial inputs as shown in Table II. The pH (pH 8.2) was measured, and it provided insight into the chemical reactivity of the water and the presence of suspended solids were observed, indicating that a portion of the material was still particulate in nature rather than fully dissolved.

Analysis of dissolved metals showed the presence of calcium (Ca^{2+}), magnesium (Mg^{2+}), sodium (Na^{+}), potassium (K^{+}), and zinc (Zn^{2+}). These ions are commonly found in MWW due to contributions from household detergents, food residues, pipe corrosion, and minor industrial discharges. Calcium and magnesium are typically associated with hardness, sodium and potassium often originate from domestic

sources such as cleaning agents and personal care products, and zinc is often introduced through plumbing systems, galvanized fittings, or minor industrial effluent [8].

Anion analysis confirmed the presence of common inorganic species, including phosphate, which often results from detergents, industrial inputs, and biological activity within the sewer system.

TABLE II. BASELINE CONCENTRATIONS OF SELECTED IONS AND PHOSPHATE IN RAW MUNICIPAL WASTEWATER.

Ion/Species	Concentration (mg/L)
Ca	4.29
Mg	0.58
Na	50.76
K	97.48
Zn	0.17
PO_4^{3-}	120.29

The raw MWW contained elevated concentrations of potassium (97.48 mg/L) and sodium (50.76 mg/L), while calcium and magnesium were comparatively low at 4.29 mg/L and 0.58 mg/L, respectively. The phosphate concentration (120.29 mg/L) indicated a high nutrient load typical of municipal effluents, supporting the need for chemical precipitation treatment. Trace levels of zinc (0.17 mg/L) were also detected, consistent with reported ranges in urban wastewater [9].

3.2. Treated Wastewater Quality After $Ca(OH)_2$ Dosing

To evaluate treatment quality effectively, phosphate and key cations including calcium (Ca^{2+}), magnesium (Mg^{2+}), sodium (Na^{+}), potassium (K^{+}), and zinc (Zn^{2+}) were selected as primary indicators. Phosphate was prioritised because it represents both an environmental liability when discharged untreated and a valuable resource if recovered successfully. Monitoring its removal or transformation provides a direct measure of the waste removal efficiency of the process [10]. Calcium and magnesium were chosen because they drive the formation of stable phosphate precipitates such as calcium phosphate and magnesium phosphate, which directly reflect the efficiency of the dosing strategy [11].

Sodium and potassium were included because, although less effective at forming precipitates, they influence the ionic balance of the water and can interfere with precipitation reactions by competing for phosphate or affecting solubility equilibria [12]. Zinc, while typically present at lower concentrations, was analyzed because it can form zinc phosphate under certain conditions and its presence also indicates contributions from industrial wastewater sources, making it a useful tracer of overall metal removal performance [13].

3.3. Phosphate Removal Efficiency

Alkaline dosing markedly treated the MWW as evident in the filtrate quality with respect to phosphate and selected cations. In the wastewater, calcium hydroxide achieved near-complete phosphate removal (≥95–100%).

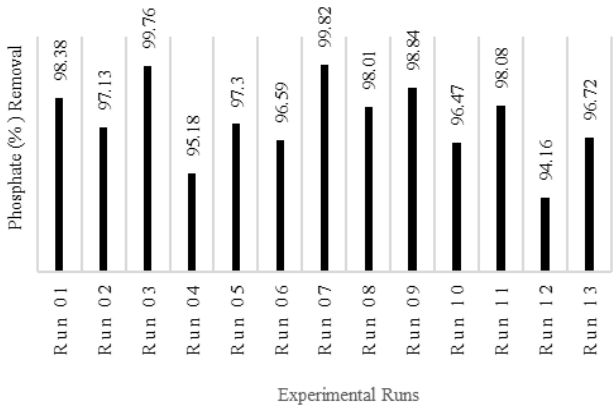

Fig. 1. Total percentage (%) removal of phosphate in MWW after treatment with $Ca(OH)_2$.

Phosphate removal across the thirteen experimental runs was consistently high, with efficiencies ranging from 94% to 99.8%, demonstrating the strong potential of calcium hydroxide as an effective precipitating agent for phosphate in MWW. The highest phosphate removals were achieved at a $Ca(OH)_2$ dosage of 3.0 g/L, a mixing speed of 125 rpm, and a contact time of 10 minutes (Run 3 and Run 7). These conditions represent the optimum operational parameters, under which sufficient hydroxide ions were available to promote the rapid formation and precipitation of insoluble calcium phosphate compounds, primarily hydroxyapatite.

The pronounced influence of chemical dosage on phosphate removal aligns with established findings in literature, which highlight calcium ion concentration as the key determinant of precipitation efficiency [7], [14]. Increasing $Ca(OH)_2$ dosage enhances supersaturation and promotes nucleation of calcium phosphate crystals, while excessive mixing or extended contact time beyond the optimal levels provides minimal additional benefit [15]. This suggests that the reaction is chemically controlled rather than kinetically limited, occurring rapidly once sufficient Ca^{2+} ions are present under alkaline conditions.

The moderate mixing speed of 125 rpm proved sufficient to ensure homogeneous dispersion of the reagent without disrupting the flocculation process, corroborating previous studies indicating that excessive agitation may hinder crystal growth and aggregation [16]. Furthermore, the relatively short contact time (10 min) associated with high removals suggests that phosphate precipitation with $Ca(OH)_2$ is a fast and efficient process, making it suitable for practical, low-cost MWW treatment applications.

3.4. Metal Ion Removal Efficiency

When $Ca(OH)_2$ is added to MWW, the resulting rise in pH promotes a range of precipitation and flocculation reactions that influence how different metal ions partition between the solid and liquid phases. Because each metal has distinct solubility characteristics under alkaline conditions, their behavior can vary noticeably across different treatment settings. To understand these differences, the removal efficiencies for the major metal ions were quantified following each experimental run, as summarized in Table III below.

TABLE III. TOTAL PERCENTAGE (%) REMOVAL OF METAL IONS IN MWW AFTER TREATMENT WITH $CA(OH)_2$.

Run	pH (after treatment)	Ca (%)	K (%)	Mg (%)	Na (%)	Zn (%)
1	12.1	-1120.5	85.5	57.2	0.0	32.3
2	11.4	-391.	85.1	74.9	0.0	95.7
3	12.0	-5940.5	82.7	81.9	-0.1	97
4	11.9	-3693.4	83.1	26	-0.2	11
5	12.1	-5056.6	83.8	84.5	0.0	54.6
6	11.9	-3599.8	83.3	53.5	0.0	28.7
7	12.3	-6317.9	84.6	81.1	-0.1	15.7
8	12.1	-5275.3	84.3	91.5	-0.1	43.9
9	12.2	-2029.4	85.5	72.6	-0.5	66.8
10	11.6	-1352.3	85.9	86.9	0.1	87.3
11	11.7	-77.0	87.4	92.0	0.0	59.6
12	11.9	52.6	87.0	89.7	-0.1	59.9
13	11.6	-3.2	87.4	96	-0.3	35.4

The metal-removal results correspond closely with the pH conditions generated by $Ca(OH)_2$ dosing, indicating that contaminant behavior in MWW is primarily governed by the extent of alkalization. Since the initial pH was 8.2, all treatments shifted the system into a strongly alkaline range (pH 11.38–12.32), where hydroxide precipitation and co-precipitation reactions dominate. Calcium showed negative removal in nearly all runs because $Ca(OH)_2$ dissolution introduces Ca^{2+} into solution, and only one condition (Run 12) achieved net positive removal. This outcome is expected: lime addition initially increases soluble calcium before equilibrium-driven re-precipitation occurs, typically as $CaCO_3$ or calcium−phosphate solids, provided that sufficient ageing and mixing are achieved [14]. The fact that Run 12 combined moderate pH (11.9) with long contact time and strong mixing suggests that calcium re-precipitation requires both adequate supersaturation and sufficient time for crystal growth.

Magnesium removal increased markedly as pH rose, in line with the well-established solubility behavior of $Mg(OH)_2$, which forms efficiently at pH values above 10.5 [17]. The highest Mg removal (96%) occurred at pH 11.6, confirming that magnesium hydroxide precipitation is successful even without the highest pH values, provided that nucleation and solid–liquid separation are favorable. Runs with very high pH (>12) but shorter contact times showed lower Mg removal, suggesting that pH alone is not sufficient; adequate residence time is needed to allow $Mg(OH)_2$ flocs to mature and settle.

Zinc removal was highly sensitive to pH, dosage, and hydrodynamic conditions. The best-performing runs (2, 3, 10, and 11) all reached pH values between 11.4 and 12.0 and achieved ≥59% zinc removal, with Run 3 exceeding 97%. This behavior is characteristic of zinc hydroxide precipitation, which becomes highly favorable at pH > 10 and proceeds rapidly at elevated

supersaturation (Fu and Wang, 2011). However, some runs with very high pH (≥12.1) showed poor zinc removal, suggesting that excessive lime dosage or overly fast mixing may inhibit particle growth or cause re-suspension, reducing settling efficiency.

Potassium (K^+), despite being a highly soluble monovalent cation, showed unexpectedly high apparent removal efficiencies (≈ 82–87%) across treatments. This behavior is consistent with reports that monovalent ions although not prone to chemical precipitation at high pH can be removed indirectly through floc entrapment, occlusion, or adsorption onto newly formed product flocs during lime treatment [4], [16]. In contrast, sodium (Na^+) exhibited negligible or even negative removal, aligning with its well-established thermodynamic stability and lack of insoluble hydroxide or carbonate formation under alkaline conditions [18] The removal trends therefore reflect physical capture mechanisms affecting K^+ but not Na^+, with K^+ removals clustering more strongly around high-pH conditions where floc volumes are known to increase and enhance particulate enmeshment.

Considering the performance across all contaminants and the corresponding pH values, the most balanced and effective condition was Run 12 (pH 11.9), which was the only run to achieve positive calcium removal while also sustaining high removal of magnesium, sodium, potassium, and zinc. This suggests that extreme pH (>12) may not be ideal for multi-metal removal; instead, a moderately high pH around 11.8–12.0, combined with sufficient mixing and contact time, provides the optimal window for simultaneous contaminant removal.

3.5. Combined Treatment Performance

To assess overall treatment efficiency, both phosphate and metal ion removal data were integrated to identify representative operating conditions for $Ca(OH)_2$ treatment. Each run was evaluated based on total contaminant removal and operational parameters. As shown in Table IV, Run 3 achieved the highest overall removal efficiency, representing the best condition, while Run 7 showed moderate performance and Run 12 the lowest. These three runs were selected for further residue characterization to illustrate how varying operational conditions influence precipitation efficiency and solid formation behavior, following approaches recommended in similar studies [14], [15].

TABLE IV. SUMMARY OF COMBINED PHOSPHATE AND METAL REMOVAL EFFICIENCIES AND CLASSIFICATION OF OVERALL PERFORMANCE.

Classification	Run	PO_4^{3-} Removal (%)	Overall Metal Removal	Remarks
Best	3	≈99.8	High	Optimum balance of chemistry
Moderate	7	≈99.7	Moderate	Good but less homogeneous mixing
Worst	12	≈94.2	Low	Affected by Over-mixing and low dosage

The integrated results demonstrate that the optimum treatment condition for simultaneous removal of phosphate and metals was achieved at 3.0 g/L $Ca(OH)_2$, 125 rpm, and 10 minutes contact time (Run 3). These parameters promoted effective precipitation of both phosphate (as hydroxyapatite) and metal ions (as hydroxides) under strongly alkaline conditions [14], [19]. The moderate run (Run 7) yielded

comparably high phosphate removal but slightly lower metal reduction due to limited mixing, while the least efficient run (Run 12) showed reduced performance, likely resulting from excessive agitation that hindered floc formation [4]

These three representative runs; best, moderate, and worst were selected for analytical characterization of the residues, as they effectively capture the influence of operational parameters across performance extremes. Characterizing their solid residues provides valuable insights into the mineralogical composition, metal incorporation, and structural stability of the precipitated products, which are crucial for understanding treatment mechanisms and potential resource recovery applications [14], [15].

3.6. Analytical Characterization of Precipitates

Two complementary analytical techniques were employed to characterize the precipitates formed during the treatment of MWW with $Ca(OH)_2$. X-ray Fluorescence (XRF) spectroscopy was used to quantify the elemental composition of the precipitates, providing insight into both major and trace elements present in the wastewater byproducts. In addition, Scanning Electron Microscopy (SEM) coupled with Energy Dispersive X-ray Spectroscopy (EDS) allowed for detailed examination of the precipitates' spatial distribution of elements within them. The combination of these techniques offers a comprehensive understanding of the composition of the precipitates, thereby elucidating the chemistry of the removed residues.

3.7. XRF Characterization of Precipitates

XRF analysis was performed to determine the elemental composition of the precipitates obtained from the selected treatment runs. Emphasis was placed on quantifying phosphate and metal ions removal under varying $Ca(OH)_2$ treatment conditions. The results shown in Table V below provide insight into the mechanisms of contaminant capture and solid-phase formation, supporting the identification of optimal treatment parameters for MWW remediation.

TABLE V. ELEMENTAL COMPOSITION (MASS %) OF PRECIPITATES FROM SELECTED RUNS DETERMINED BY XRF.

Component	Run 03	Run 07	Run 12
MgO	10.19	0.34	0.33
Al_2O_3	0.49	0.19	0.16
SiO_2	1.3	0.62	0.43
P_2O_5	36.74	13.72	2.13
SO_3	2.02	0.53	0.43
Cl	0.32	0.26	–
K_2O	0.49	0.12	0.11
CaO	40.12	82.55	95.17
Cr_2O_3	0.82	0.28	–
MnO	0.26	–	–
Fe_2O_3	1.33	0.93	0.84
NiO	0.15	–	0.1
CuO	0.46	–	0.07
ZnO	5.26	0.32	0.12

SrO	0.07	0.15	0.12
Na_2O	–	–	0.01

The XRF profiles reveal that Run 03, corresponding to the highest removal efficiency, produced a precipitate rich in P_2O_5 (36.7 %) and moderate CaO (40.1 %), indicating extensive phosphate precipitation primarily as calcium phosphate species. The elevated presence of ZnO (5.26 %) and MgO (10.19 %) suggests significant co-precipitation of metal hydroxides, consistent with the enhanced removal observed under optimal treatment conditions [20], [21].

In contrast, Run 07 and Run 12 exhibited very high CaO content (82–95 %) signifying a predominance of unreacted or excess lime residues. This trend implies that while higher $Ca(OH)_2$ dosages increase alkalinity, excessively short contact times or suboptimal mixing can limit phosphate-metal complexation (Zhou et al., 2020).

3.8. SEM–EDS Characterization of Precipitates

SEM–EDS analysis was conducted on the solid residues from the three representative treatment runs (Run 03, Run 07 and Run 12) to examine the elemental distribution. This analysis complements the bulk elemental composition obtained from XRF and provides insight into the precipitation mechanisms operating under different $Ca(OH)_2$ treatment conditions. SEM−EDS is particularly valuable for identifying calcium phosphate phases, unreacted lime, and metal incorporation on particle surfaces [22].

The EDS spectra for Run 03 shown (Fig. 2(a)) exhibit dominant Ca and P peaks with noticeable Mg and Zn signals. This morphology and composition correspond closely with the XRF results, which showed high P_2O_5 (36.7 %) and substantial CaO, MgO and ZnO. The co-localization of Ca and P confirms the formation of calcium phosphate most likely hydroxyapatite while the presence of Mg and Zn suggests partial substitution or surface adsorption within the Ca–P lattice[14]. These observations are consistent with efficient phosphate removal and enhanced metal co-precipitation under balanced chemical and mixing conditions.

Run 07 (Fig. 2(b)) displayed predominantly smooth, lime-like particles with weaker P peaks and strong Ca signals in the EDS spectra, reflecting the high CaO (92.6 %) and moderate P_2O_5 (13.7 %) composition reported by XRF. It indicates excess unreacted $Ca(OH)_2$ and incomplete conversion to Ca-P minerals. Reduced phosphate incorporation may result from localized oversaturation of Ca^{2+} and limited contact between Ca and phosphate due to lower mixing intensity [23-25]. Similar behavior has been reported where sub-optimal mixing or excessive alkalinity limits Ca–P nucleation [19].

For Run 12 (Fig 2(c)), SEM–EDS revealed large, irregular Ca-rich agglomerates with minimal phosphorus presence, in agreement with the XRF result ($CaO \approx 95$ %, $P_2O_5 \approx 2.1$ %). The lack of well-defined Ca−P crystals and negligible metal signatures indicate that high mixing speed and prolonged contact time disrupted floc formation, reducing phosphate and metal capture efficiency [4].

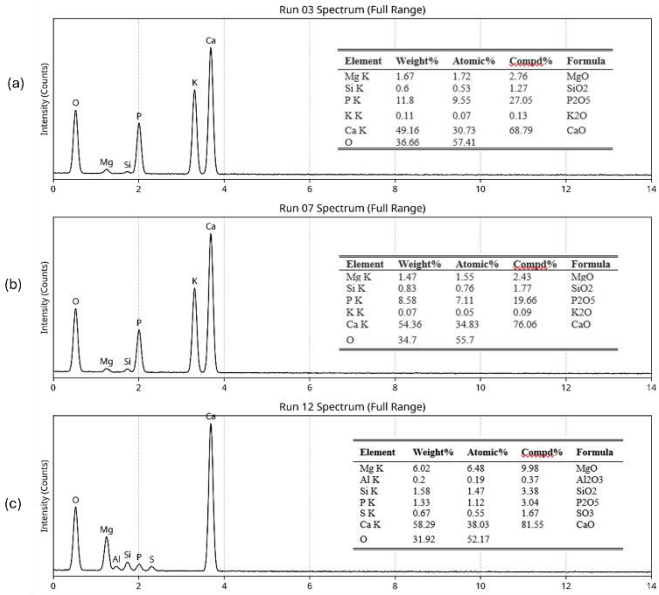

Fig. 2. SEM–EDS spectra of precipitates from (a) Run 03, (b) Run 07, and (c) Run 12, showing decreasing P and metal signals with increasing Ca dominance from the optimum to the least efficient conditions, consistent with XRF results and reflecting reduced phosphate.

4. Conclusion

This study demonstrated that calcium hydroxide can effectively remove both phosphate and metal ions from MWW, with performance strongly dependent on operational parameters. Optimal removal was achieved at a $Ca(OH)_2$ dosage of 3.0 g L^{-1}, mixing speed of 125 rpm, and contact time of 10 minutes (Run 03), which yielded near-complete phosphate precipitation and efficient co-removal of divalent metals such as Zn and Mg. XRF and SEM–EDS analyses confirmed that under these conditions, precipitates were dominated by calcium-phosphate phases enriched with incorporated metals, while less efficient runs were characterized by Ca-rich, P-deficient residues. These findings confirm that effective treatment depends on achieving appropriate Ca: P stoichiometry and controlled mixing to favor nucleation and growth of Ca–P crystals rather than accumulation of unreacted lime [14].

Overall, optimizing $Ca(OH)_2$ dosage and hydrodynamic conditions enhances both contaminant removal and precipitate quality, supporting the development of cost-effective, resource-recovery-oriented wastewater treatment strategies. The results align with previous studies highlighting lime-based systems as reliable and scalable for phosphate recovery and heavy-metal control in municipal effluents [7], [15].

5. Acknowledgment

The authors gratefully acknowledge the organizers of the 8th International Conference on Multidisciplinary Research and Innovation (ICMRI 2025), hosted by the Dynamic Research Academic and Publication House (DRAPL), for the invitation to present this research. The opportunity to share the findings and engage with fellow researchers is sincerely appreciated

6. References

[1] A. I. Abd El-Kader, M. Zaky, and M. A. El-Serafy, “Microbial Remediation of some Heavy Metals in Wastewaters of Lake Manzala, Egypt,” *Egypt J Aquat Biol Fish*, vol. 26, no. 5, 2022, doi: 10.21608/ejabf.2022.262658.
https://doi.org/10.21608/ejabf.2022.262658

[2] M. Anjum, R. Miandad, M. Waqas, F. Gehany, and M. A. Barakat, “Remediation of wastewater using various nano-materials,” 2019. doi: 10.1016/j.arabjc.2016.10.004.
https://doi.org/10.1016/j.arabjc.2016.10.004

[3] C. Kazadi Mbamba *et al.*, “Plant-wide model-based analysis of iron dosage strategies for chemical phosphorus removal in wastewater treatment systems,” *Water Res*, vol. 155, 2019, doi: 10.1016/j.watres.2019.01.048.
https://doi.org/10.1016/j.watres.2019.01.048

[4] H. H. Q. Ho, “Enhanced removal of phosphate from wastewater by precipitation coupled with flocculation,” *Journal of Science and Technology Issue on Information and Communications Technology*, 2021, doi: 10.31130/ud-jst2021-010e.
https://doi.org/10.31130/ud-jst2021-010E

[5] Y. Liu *et al.*, “Novel porous phosphoric acid-based geopolymer foams for adsorption of Pb(II), Cd(II) and Ni(II) mixtures: Behavior and mechanism,” *Ceram Int*, vol. 49, no. 4, 2023, doi: 10.1016/j.ceramint.2022.10.164.
https://doi.org/10.1016/j.ceramint.2022.10.164

[6] O. A. Bin-Dahman and T. A. Saleh, “Synthesis of polyamide grafted on biosupport as polymeric adsorbents for the removal of dye and metal ions,” *Biomass Convers Biorefin*, vol. 14, no. 2, 2024, doi: 10.1007/s13399-022-02382-8.
https://doi.org/10.1007/s13399-022-02382-8

[7] C. Nepfumbada, N. T. Tavengwa, V. Masindi, S. Foteinis, and E. Chatzisymeon, “Recovery of phosphate from municipal wastewater as calcium phosphate and its subsequent application for the treatment of acid mine drainage,” *Resour Conserv Recycl*, vol. 190, 2023, doi: 10.1016/j.resconrec.2022.106779.
https://doi.org/10.1016/j.resconrec.2022.106779

[8] S. A. Parsons and J. A. Smith, “Phosphorus removal and recovery from municipal wastewaters,” *Elements*, vol. 4, no. 2, 2008, doi: 10.2113/GSELEMENTS.4.2.109.
https://doi.org/10.2113/GSELEMENTS.4.2.109

[9] Renu, M. Agarwal, and K. Singh, “Heavy metal removal from wastewater using various adsorbents: A review,” 2017. doi: 10.2166/wrd.2016.104.
https://doi.org/10.2166/wrd.2016.104

[10] L. E. De-Bashan and Y. Bashan, “Recent advances in removing phosphorus from wastewater and its future use as fertilizer (1997-2003),” *Water Res*, vol. 38, no. 19, 2004, doi: 10.1016/j.watres.2004.07.014.
https://doi.org/10.1016/j.watres.2004.07.014

[11] S. Salehi, K. Y. Cheng, A. Heitz, and M. P. Ginige, “Re-visiting the Phostrip process to recover phosphorus from municipal wastewater,” *Chemical Engineering Journal*, vol. 343, 2018, doi: 10.1016/j.cej.2018.02.074.
https://doi.org/10.1016/j.cej.2018.02.074

[12] M. K. Perera and J. D. Englehardt, “Simultaneous nitrogen and phosphorus recovery from municipal wastewater by electrochemical pH modulation,” *Sep Purif Technol*, vol. 250, 2020, doi: 10.1016/j.seppur.2020.117166.

[13] A. RoyChowdhury, D. Sarkar, and R. Datta, “Removal of Acidity and Metals from Acid Mine Drainage-Impacted Water using Industrial Byproducts,” *Environ Manage*, vol. 63, no. 1, 2019, doi: 10.1007/s00267-018-1112-8.
https://doi.org/10.1007/s00267-018-1112-8

[14] Y. Li, Y. Chen, J. Xu, and J. Liu, “Removal mechanism of phosphorus in water by calcium hydroxide modified copper tailings,” *Sci Rep*, vol. 14, no. 1, Dec. 2024, doi: 10.1038/s41598-024-71347-w.
https://doi.org/10.1038/s41598-024-71347-w

[15] S. Sengupta, T. Nawaz, and J. Beaudry, “Nitrogen and Phosphorus Recovery from Wastewater,” Sep. 01, 2015, *Springer*. doi: 10.1007/s40726-015-0013-1.
https://doi.org/10.1007/s40726-015-0013-1

[16] H. N. S. Wiechers, “Chemical phosphate removal from municipal waste waters: Current practice and recent innovations,” *Water SA*, vol. 12, no. 4, 1986.

[17] R. C. Carson and J. Simandl, “Kinetics of magnesium hydroxide precipitation from seawater using slaked dolomite,” *Miner Eng*, vol. 7, no. 4, 1994, doi: 10.1016/0892-6875(94)90164-3.
https://doi.org/10.1016/0892-6875(94)90164-3

[18] U. Zulfiqar, T. Subhani, and S. Wilayat Husain, “Synthesis of silica nanoparticles from sodium silicate under alkaline conditions,” *J Solgel Sci Technol*, vol. 77, no. 3, 2016, doi: 10.1007/s10971-015-3950-7.
https://doi.org/10.1007/s10971-015-3950-7

[19] C. Nepfumbada, N. T. Tavengwa, V. Masindi, S. Foteinis, and E. Chatzisymeon, “Recovery of phosphate from municipal wastewater as calcium phosphate and its subsequent application for the treatment of acid mine drainage,” *Resour Conserv Recycl*, vol. 190, Mar. 2023, doi: 10.1016/j.resconrec.2022.106779.
https://doi.org/10.1016/j.resconrec.2022.106779

[20] C. Xu, R. Liu, and L. Chen, “Removal of Phosphorus from Domestic Sewage in Rural Areas Using Oyster Shell-Modified Agricultural Waste–Rice Husk Biochar,” *Processes*, vol. 11, no. 9, 2023, doi: 10.3390/pr11092577.
https://doi.org/10.3390/pr11092577

[21] T. T. Dai *et al.*, “PERFORMANCE AND MECHANISM OF PHOSPHORUS REMOVAL BY CALCIUM-LOADED CLAY GRANULAR ADSORBENTS,” *Appl Ecol Environ Res*, vol. 22, no. 1, 2024, doi: 10.15666/aeer/2201_9971012.
https://doi.org/10.15666/aeer/2201_9971012

[22] M. R. Senra, R. B. de Lima, D. de H. S. Souza, M. de F. V. Marques, and S. N. Monteiro, “Thermal characterization of hydroxyapatite or carbonated hydroxyapatite hybrid composites with distinguished collagens for bone graft,” *Journal of Materials Research and Technology*, vol. 9, no. 4, 2020, doi: 10.1016/j.jmrt.2020.04.089.
https://doi.org/10.1016/j.jmrt.2020.04.089

[23] Elvis Fosso-Kankeu, Alusani Manyatshe, Frans Waanders. 2017. Mobility potential of metals in acid mine drainage occurring in the Highveld area of Mpumalanga Province in South Africa: Implication of sediments and efflorescent crusts. International Biodeterioration and Biodegradation. 119: 661-670.
https://doi.org/10.1016/j.ibiod.2016.09.018

[24] Vhahangwele Masindi, Elvis Fosso-Kankeu, Ednah Mamakoa, Thabo T.I. Nkambule, Bhekie B. Mamba, Mu. Naushad , Sadanand Pandey. 2022. Emerging remediation potentiality of struvite developed from municipal wastewater for the treatment of acid mine drainage. Environmental Research. 210: 112944. doi.org/10.1016/j.envres.2022.112944.
https://doi.org/10.1016/j.envres.2022.112944

[25] Sadanand Pandey, Elvis Fosso-Kankeu, Johannes Redelinghuys, Joonwoo Kim, Misook Kang. 2021. Implication of biofilms in the sustainability of acid mine drainage and metals dispersion near coal tailings. Science of The Total Environment. 788: 147851. https://doi.org/10.1016/j.scitotenv.2021.147851.[4] E Fosso-Kankeu. 2018. Synthesized af-PFCl and GG-g-P(AN)/TEOS hydrogel composite used in hybridized technique applied for AMD treatment. Journal of Physics and Chemistry of the Earth. 105: 170-176.
https://doi.org/10.1016/j.scitotenv.2021.147851